ORNL
MASTER COPY

DATE ISSUED DEC 15 1980

OAK RIDGE NATIONAL LABORATORY
OPERATED BY
UNION CARBIDE CORPORATION
NUCLEAR DIVISION

POST OFFICE BOX X
OAK RIDGE, TENNESSEE 37830

SPECIAL DISTRIBUTION

ORNL
CENTRAL FILES NUMBER
ORNL/CF-80/349

801204

DATE: December 4, 1980

SUBJECT: Technical Highlights of Space and Terrestrial Systems Programs at Oak Ridge National Laboratory for July 1980

TO: Distribution

FROM: R. H. Cooper

This monthly report is intended to inform the Space and Terrestrial Systems Division, DOE, and their contractors of significant technical highlights of technology and systems support programs in progress at Oak Ridge National Laboratory. A detailed technical presentation of information will be published in topical reports and open literature publications.

[redacted]

CONTENTS

SOLAR-POLAR MISSION MATERIALS SUPPORT 1

CBCF Insulation Fabrication 1
CBCF-3 Characterization 3
Creep Properties of 2219 Aluminum Housing Materials 7

FLIGHT SYSTEMS HARDWARE 12

Iridium Blank Fabrication 12
Iridium Foil Fabrication 12
Iridium Management 13
Meetings 13

MATERIALS TECHNOLOGY SUPPORT 14

Tensile Properties of DOP-26 14
AES Analysis of P-Doped DOP-26 14
AES Analyses of S-Doped DOP-26 15
Characterization of DOP-26 Ir—0.3% W Production Sheet 15
Impact Properties of Pt—30% Rh 16

ISOTOPE FUEL DEVELOPMENT 19

$^{90}SrF_2$ Compatibility 19

TERRESTRIAL RADIOISOTOPE APPLICATION DEVELOPMENT 20

Cesium-137 Low Solubility Compounds 20
Krypton-85 Light Source Development 22

BENEFICIAL APPLICATIONS OF RADIATION TECHNOLOGY 23

SOLAR-POLAR MISSION MATERIALS SUPPORT

(Activity AE 15 15 20 0, WPAS 02313)

R. L. Heestand

The purpose of this task is to provide direct materials support on work specific to the General Purpose Heat Source (GPHS) design. The scope of this work includes (1) determining the impact properties and optimum weld parameters for the DOP-26 iridium alloy fuel cladding material, (2) thermal conductivity and emissivity data on cladding and thermal insulation materials, (3) fabrication and characterization of test samples of carbon-bonded carbon-fiber (CBCF) insulation developed by ORNL and Y-12 which may be used for GPHS, and (4) determination of creep properties of the 2219 aluminum alloy housing. Data on the impact properties and welding of iridium are integrated with complementary work reported in the Materials Technology section of this report.

CBCF Insulation Fabrication (J M Robbins and G. C. Wei)

Two rough machined tubes, C-6-2 and C-6-4, previously shipped to LASL for final machining and use in the CET, were rejected when returned to ORNL for radiographic inspection. Both parts had more and larger voids than did C-6-5 which was used in the GE vibration test. Consequently, the two spare parts, C-15-4 and C-15-7, from the GE vibration test will be substituted for the CET.

Two rough machined billets, C-16-1 and C-16-5, have been shipped to LASL for impact test No. 2. Five sleeves that have been final machined at ORNL, are currently being dimensionally and visually inspected by the ORNL Inspection Department. Three of these sleeves, C-20-2, C-20-3, and C-20-4 will be shipped to LASL for use in their impact test Nos. 3 and 4, and the other two sleeves, C-20-6 and C-20-8, will be shipped for use in the LASL aging experiment. Finally, billets C-16-9 and C-20-1 have been rough machined and are available to meet future CBCF testing needs.

In addition to the parts fabricated and shipped for the various tests as reported above, six sets of final machined parts, that were fabricated earlier at the Y-12 plant, were dimensionally inspected and shipped to Mound Laboratories for their use in evaluating their dimensional measurement facilities. As stated, these parts were fabricated earlier at the Y-12 plant and will not be certified as flight quality hardware.

Part yield continues to be a problem due to cracking evident after the carbonization process. Slower heatup rates during the process doesn't seem to be the total answer. Currently, the drying and curing cycle is being studied to see if stresses are being generated during the rather fast two-step curing process.

Density variation is the single most pressing problem at present. These variations have been noted from run to run as well as within a single run. In general, these variations range from about 0.21 to 0.26 Mg/m^3 and are greater from run to run than they are within a single run. The dewatering step is being investigated as the possible cause of the density variation. Earlier experience at the Y-12 plant showed that varying amounts of water left in the parts at the beginning of the drying and curing cycle would cause different degrees of shrinkage during polymerization resulting in density variation. It was also noted earlier that the ideal water to solids ratio after dewatering ranged from 1:1 to 0.7:1. However, a water to solids ratio of less than 1.3:1 is very difficult or impossible to achieve in a reasonable dewatering time with the equipment now on hand. Replacement of the present pumping system with a more appropriate one seems mandatory, therefore a suitable pump is being purchased.

The radiographic quality of the latest CBCF parts are significantly better than some of the parts fabricated earlier. High density inclusions and voids are the most notable defects revealed by radiography. The large (in size and number) voids noted in the past have been reduced to an acceptable level. This was accomplished by modifying the process and technique to minimize bubble and foam formation during slurry transfer and molding. High density inclusions have been minimized by filtering the molding water, carefully cleaning molding equipment before each use, and by carefully avoiding contamination. It should be pointed out that the fabricated part involved here has a density of about 0.22 Mg/m^3 so that just about anything will show up radiographically as a high density inclusion when compared to the density of the part. High density inclusions could be pieces of carbon or graphite etc. and do not necessarily imply metallic inclusions. Occasionally a large number of inclusions are observed in a single part during a molding run (C-16 for instance). This isn't understood since nine parts are being molded simultaneously from a common molding tank. The only explanation to be offered is the possibility of the stockinette filter on one particular mold being contaminated. In any case, it is felt that voids and high density inclusions have been reduced to an acceptable level.

CBCF-3 Characterization (G. C. Wei)

Thermal conductivity specimens from six CBCF-3 cups (with two each from three multimandrel runs) and two CBCF-3 plates fabricated at Y-12 and carbonized at 1350°C for 3 h and outgassed (1500°C/36 h/5.0E-5 torr) were sent to TPRL of Purdue University for thermal conductivity determinations. These specimens have densities ranging from 0.18 to 0.22 E3 kg/m^3. Results of the thermal conductivity measurements are shown in Table 1. At 2000°C, the thermal conductivities fall into the range from 0.12 to 0.24 W/m·K. The room-temperature thermal conductivities vary from 0.0222 to 0.0513 W/m·K. Additional thermal conductivity specimens from CBCF-3 billets fabricated at ORNL and carbonized at 1600°C for 3 h have been delivered to Purdue and results are due on August 26, 1980.

Chemical analyses including ash analysis and spark source mass spectroscopic analysis of outgassed CBCF-3 materials fabricated at ORNL were performed. The results of ash analyses of outgassed samples from CBCF-3 tubes: C-1-1, C-2-6, C-6-1, C-7-1, C-8-7, C-9-9, C-10-9, C-11-1, C-12-1, C-6-5, C-15-2, C-15-4, C-15-7, and CBCF-3 plate P-C-2 indicated the ash contents all less than 0.3% as specified in Mound Facility's CBCF-3 specification. Spark source mass spectroscopic chemical analyses of outgassed samples from ORNL-fabricated CBCF-3 tubes C-6-3, C-7-1, and C-8-7 showed concentrations of all elements within the specification limits. Spark source chemical analyses of nine other samples are in process.

The bulk densities of ORNL-fabricated CBCF-3 tubes and plates were determined. The results are shown in Table 2. All the CBCF-3 parts meet the density specification (0.20 ± 0.02 E3 kg/m^3) except tubes C-18s and C-20s and plate P-3s. The cause of the deviation of the densities (0.23–0.26 E3 kg/m^3) of tubes C-18s, C-20s, and plate P-3s from the specification (0.20 ± 0.02 E3 kg/m^3) is presently unknown and being investigated.

The compressive strengths of outgassed test samples from tubes C-15-2, 4, 7, C-6-5, and plate P-C-2 were measured to be within the specification (>0.52 MPa). Test specimens from other billets are being outgassed for compressive strength testings.

Dimensional stability of CBCF-3 tubes C-9-5 and C-9-9 during the 1500°C/36 h/5.0E-5 torr outgassing was studied. No measurable changes in dimensions were observed during the outgassing.

In this period, post-vibration CBCF-3 sleeves 1682 and 1680 and disks 1732, 1733, 1734, and 1735 were examined. Major conclusions were: (1) sleeve 1682 failed probably because GIS pounding CBCF-3 against aeroshell; rotation, rattling, and rubbing of CBCF-3 against aeroshell and between two CBCF-3 sleeves; tilt of GIS to produce shear on CBCF-3 sleeve; (2) the outer diameter and length of CBCF-3 sleeves should be modified and possibly increased to prevent rattling of CBCF-3 sleeve during vibration. The results of the examinations were presented at a status review meeting at ORNL on July 31, 1980.

Table 1. Thermal Conductivity Results of CBCF-3

Sample	Density (E3 kg/m^3)	Temperature (°C)	Environment	Thermal Conductivity (W/m·K)
Cup 98	0.196	23	Vacuum	0.0222
Cup 98	0.196	2000	Vacuum	0.139
Cup 78	0.209	23	Vacuum	0.0582
Cup 78	0.209	2000	Vacuum	0.234
Cup 94	0.181	23	Vacuum	0.0222
Cup 94	0.181	2000	Vacuum	0.128
Cup 100	0.216	23	Vacuum	0.0511
Cup 100	0.216	2000	Vacuum	0.232
Cup 101	0.192	23	Vacuum	0.0386
Cup 101	0.192	2000	Vacuum	0.202
Cup 119	0.200	23	Vacuum	0.0394
Cup 119	0.200	2000	Vacuum	0.215
Plate 1	0.202	23	Vacuum	0.0444
Plate 1	0.202	2000	Vacuum	0.217
Plate 4	0.224	23	Vacuum	0.0513
Plate 4	0.224	2000	Vacuum	0.241

Table 2. Density of ORNL-Fabricated CBCF-3 Parts

Part No.	Density (g/cc)		
	Test Samples	Pre-Machined Billet	Final Machined Part
C-1-1	—	0.224	—
C-2-1	—	0.214	—
C-6-1	—	0.201	—
C-6-2	0.219 0.214 0.216 0.221	0.225	—
C-6-4	0.215 0.215 0.214 0.218	0.222	—
C-6-5	0.213 0.222	0.222	—
C-6-6	0.220 0.224 0.227 0.219	0.224	—
C-7-1	—	0.209	—
C-8-7	—	0.217	—
C-8-8	—	0.218	—
C-8-1	0.223 0.216 0.221 0.226	—	—
C-8-2	0.214 0.209 0.218 0.212	—	—
C-8-3	0.216 0.223 0.217 0.216	—	—

Table 2. (continued)

Part No.	Density (g/cc)		
	Test Samples	Pre-Machined Billet	Final Machined Part
C-8-4	0.215 0.213 0.220 0.223	—	—
C-8-5	0.207 0.217 0.220 0.210	—	—
C-8-6	0.219 0.222 0.219 0.215	—	—
C-9-5	—	0.206	—
C-9-9	—	0.204	—
C-10-8	—	0.215	—
C-10-9	—	0.213	—
C-15-2	0.219-0.230	0.222	—
C-15-4	0.216-0.223	0.222	—
C-15-7	0.219-0.222	0.221	—
P-C-2	0.210-0.218	—	—
P-3-2	0.238-0.251	—	—
C-16-1	0.207-0.220	—	—
C-16-5	0.211-0.220	—	—
C-16-9	0.208-0.215	—	—
C-20-1	0.234-0.240	—	—
C-20-2	0.229-0.236	—	0.240
C-20-3	0.230-0.238	—	0.237
C-20-4	0.233-0.244	—	0.238
C-20-6	0.233-0.236	—	0.239
C-20-8	0.228-0.237	—	0.241
C-18-6	0.241-0.247	—	—
C-18-7	0.235-0.250	—	—
P-3-1	0.237-0.260	—	—

Creep Properties of 2219 Aluminum Housing Materials (J. P. Hammond)

The purpose of this task is to develop creep design curves on the 2219-T6 aluminum forging and to aid GE, Valley Forge, in the design of the shell component of the RTG generator. The essential requirement of the shell will be to firmly retain the RTG generator under elastic stress during ground tests and storage in air (condition II), and subsequent flight in vacuum (condition I).

Test specimens were provided from the end cropping of the 2219-T6 forging from which the shell will be fabricated and GE communicated an agreed-on creep test matrix, given in the last report.[1] The status of the creep tests conducted to date are given in Table 3. Total creep strain (ε_p) for the time in test (t) are given along with the constant rate of secondary creep ($\dot{\varepsilon}_m$). Since approximately 700 h additional time has been logged in on these tests since the time of last reporting, the $\dot{\varepsilon}_m$ values generally are somewhat more reliable than before.

The computer readout creep graphs for proof tests II and I of Table 3, which are intended to evaluate the magnitude of creep strain under worst stress-temperature conditions during the 10,500 h testing and storage on ground and 10,000 h flight in space, respectively, are reproduced in Fig. 1 and 2. It is understood that the primary creep in Fig. 1 (AB+CD) will be largely compensated for by selective design and operation of the unit and that secondary creep will be the major concern. Whereas a previous measurement had given a minimum creep rate of 1.5×10^{-5}%/h for proof test II, the present value is 0.92×10^{-5}%/h. The latter corresponds to about 0.1% creep in 10,000 h. For proof test I, the earlier $\dot{\varepsilon}_m$ value was 6.6×10^{-5}%/h but now is 4.7×10^{-5}%/h or 0.47% creep in 10,000 h. The 0.1% creep during storage on the ground appears to be a manageable figure but 0.47% creep during the space flight seems somewhat excessive and it may be desirable to reduce stress in order to reduce the extent of this strain. The impact of such creep numbers on the present design is being examined by GE.

The extent to which the 0.09% primary creep indicated in Fig. 2 (AB) will be realized during the transition from the ground conditions to space flight conditions is not known at present. It is planned to determine this by placing the test specimen of proof test II under the stress (σ) and temperature of proof test I to establish this, once proof test II is completed. An important facet of these proof tests will be to determine whether the constant rates of creep measured early in the tests are maintained throughout the 10,000 h period. Whether they do or not will depend upon how structurally stable the alloys remain during test.

---

[1]Monthly Highlights, June 1980.

Additional data points were obtained from the tests of Table 3 to extend the 260°C design curves (log σ - log t for 0.1 and 0.2% ε_p) to longer times. Whereas the data give reasonably straight curves for periods of time to 100 to 1000 h, data beyond 1000 h suggest a possible deflection downward to lower σ values. This feature adds to the inconsistency of the primary creep behavior of this alloy already cited.[1]

A plotting of the 260°C minimum creep rate data of Table 3* as a log σ - log $\dot{\varepsilon}_m$ graph gave a reasonably straight curve. Extrapolation of the curve gave a stress of 3.8 ksi for 0.2% secondary creep strain and a stress of 2.8 ksi for 0.1% strain.

---

*The 270°C data point of Proof Test I was included.

Table 3. Creep Tests[a] on 2219-T6 Forging

Test	Specimen No.[b]	Temp. (°C)	Stress (ksi)	Creep, ε_p (%)	Time, t (h)	Rate, $\dot{\varepsilon}_m$ (%/h)	Status
I, Proof	LT-11	270	5.0	0.143	1627	4.69×10^{-5}	Running
II, Proof	LT-6	270	3.5	0.084	597	c	---
	LT-6	177	8.0	0.028	1560	0.92×10^{-5}	Running
III, Design	LT-7	260	9.5	0.371	979	2.15×10^{-4}	Discont.
III, Design	LT-12	260	8.2	0.338	1939	1.05×10^{-4}	Running
III, Design	LT-17	260	7.7	0.3615	1817	1.5×10^{-4}	Running
III, Design	LT-9	260	6.0	0.118	834	6.75×10^{-5}	Running
III, Design	LT-14	260	5.0	d	—	—	Running
IV, Design	LT-8	177	7.0	0.1735	929	2.25×10^{-5}	Running
IV, Design	LT-13	177	5.8	d	—	—	Running
Preliminary	L-1	260	9.5	0.154	1026	4.6×10^{-5}	Discont.
Preliminary	L-2	177	8.0	0.221	1145	1.5×10^{-5}	Discont.

[a]Conducted in air

[b]LT = long transverse orientation, L = longitudinal

[c]In primary creep stage

[d]Just started

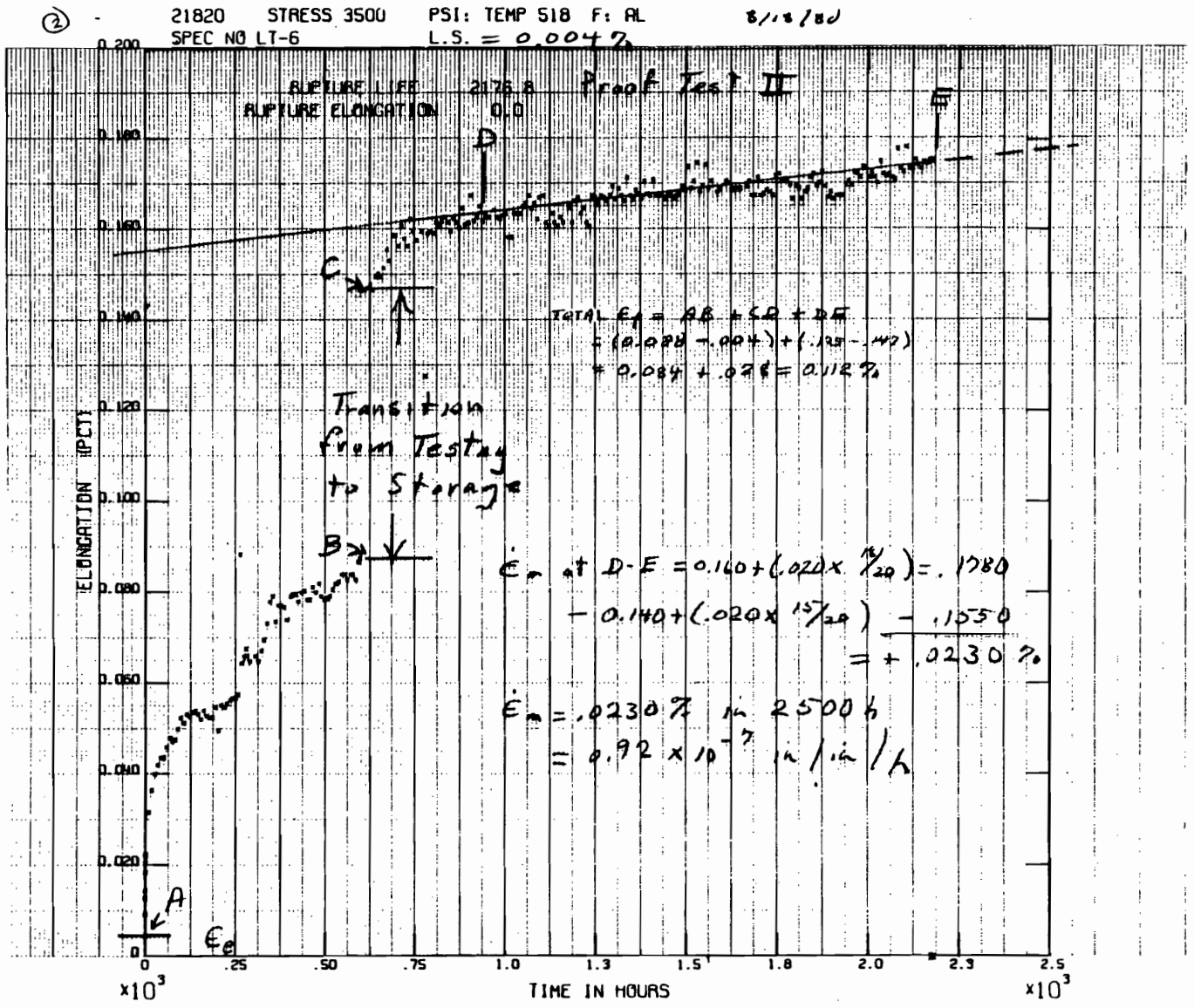

Fig. 1. Creep Response of Proof Test II.

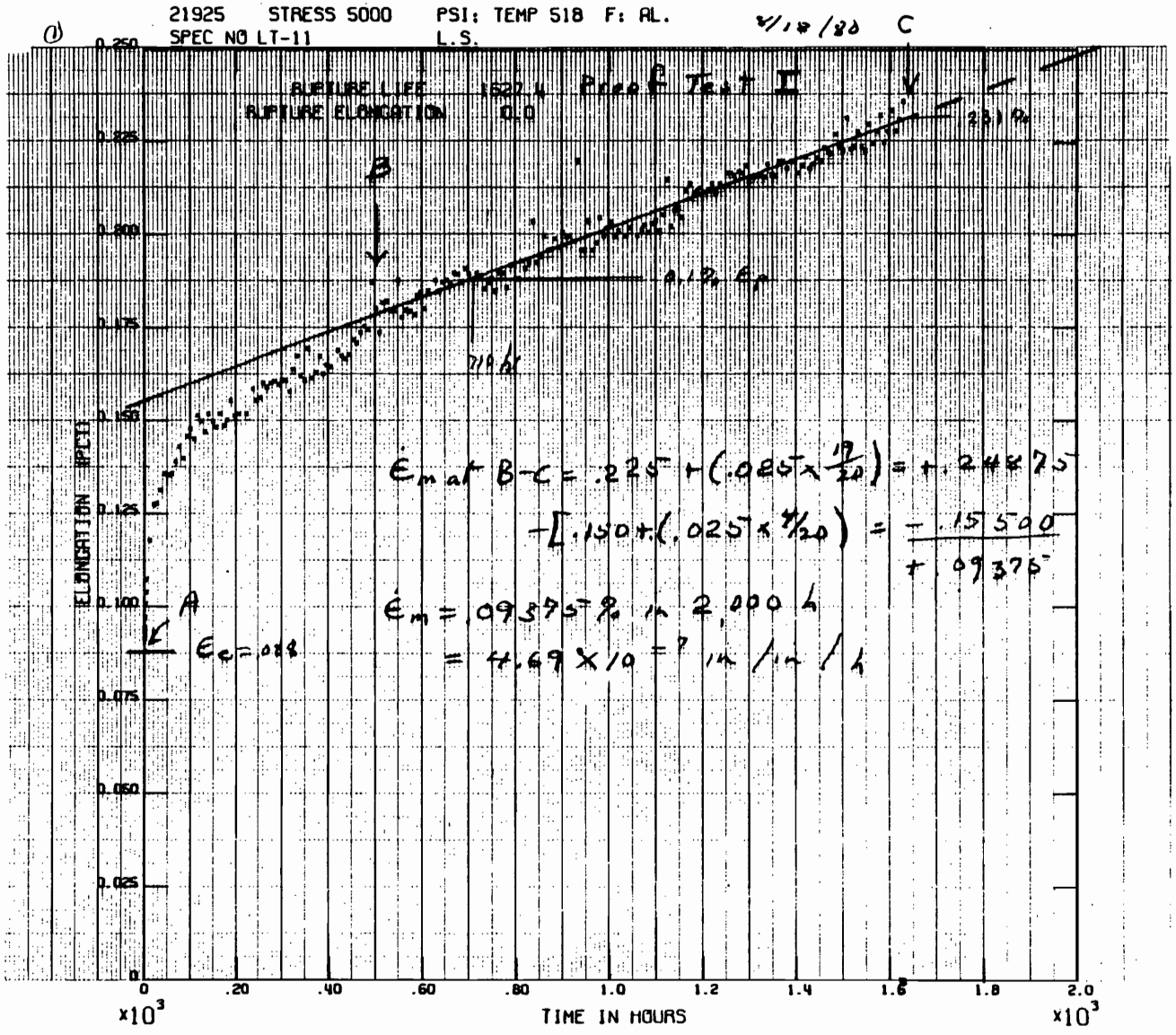

Fig. 2. Creep Response of Proof Test I.

FLIGHT SYSTEMS HARDWARE

(Activity AE 15 20 00 0, WPAS 01322)

D. E. Harasyn

The objective of this task is to supply Mound Facility with flight quality hardware components for use in the assembly of isotope heat sources. The major activity is on fabrication of iridium alloy forming blanks for isotope fuel capsules along with iridium foil for vents, decontamination covers, and weld shields. We have completed fabrication of iridium for the Galileo mission MHW heat source and have initiated fabrication 1255 iridium blanks and associated foil for Solar-Polar Mission General Purpose Heat Source for delivery in FY 1980 and FY 1981. The task on fabrication of carbon-bonded carbon-fiber (CBCF) thermal insulation for Light Weight Radioisotope Heating Units (LWRHU) has been deleted due to selection of pyrolytic graphite for the application.

Iridium Blank Fabrication (D. E. Harasyn)

Fifty-five forming blanks were shipped to MRC in July. Of the 396 blanks for GPHS production that were to have been shipped by the end of July (July 1, 1980 Integrated Master Schedule), 300 have been shipped. Discussions on the criteria for visual inspection among MRC, ORNL, GE, and DOE were continued. Acceptance of the GE proposed specification limiting defect depth to $\leq$0.001 in. and diameter $\leq$0.004 in. would require grinding of all blanks. It has also been determined that blanks which have passed dye penetrant inspection at ORNL show defects when dye penetrant inspected at MRC indicating a higher degree of sensitivity with the MRC process.

An experiment was initiated to determine the effects of surface treatment of the hot rolled iridium sheet on the incidence or defects after cold rolling. Six plates were hot rolled to the thickness where cold rolling is initiated, at this point two plates were continued through the cold rolling process with no treatment. Two plates were grit blasted prior to cold rolling and two plates were wire brushed prior to cold rolling. Results as determined by dye penetrant testing of the plates indicated that more defects were introduced by grit blasting, while the number of penetrant defects in both the as-rolled and wire brushed sheets were approximately the same as those usually found indicating no effect of the treatments.

Iridium Foil Fabrication (D. E. Harasyn)

Approximately 0.06 m^2 of FS-5 undoped Ir–0.3% W foil 0.13-mm thick was shipped to MRC.

Iridium Management (W. O. Graves and R. L. Heestand)

The iridium management plan developed to define areas of responsibilities and controls for flow of materials, funding and records for all DOE contractors, area offices, vendors, and refiners was approved by DOE-ORO. Copies of the plan were distributed to all involved parties for their review and implementation.

Requests for quote have been issued for refining 28 kg of Ir and for direct purchase of 12 kg of Ir.

Meetings

R. H. Cooper and A. C. Schaffhauser attended a GPHS review meeting at DOE, Germantown on July 1, 1980.

R. H. Cooper, A. C. Schaffhauser, and other ORNL personnel, hosted an STS program review meeting held at ORNL on July 31, and August 1, 1980.

MATERIALS TECHNOLOGY SUPPORT

(Activity AE 15 35 00 0, WPAS 01495)

C. T. Liu

The primary objective of this task is to characterize and improve the metallurgical and mechanical properties of noble base alloys, mainly DOP-26 (Ir–0.3% W doped with 60 ppm Th and 50 ppm Al), to meet the requirements of cladding material in radioisotope heat resources for the Galileo and Solar-Polar space missions. The current efforts are concentrated on four areas: (1) to characterize the impact properties of Ir alloys in the temperature range 800–1400°C, (2) to improve the low-temperature impact properties of welds in the DOP-26 alloy, (3) to identify the mechanism and sources that degrade the mechanical and metallurgical properties of doped Ir alloys under heat-source environments, and (4) to develop ductile high-temperature alloys acceptable for future flight missions.

Tensile Properties of DOP-26 (C. T. Liu)

Tensile properties of DOP-26 Ir–0.3% W were determined at temperatures to 1600°C at a crosshead speed of 0.25 cm/min. The results of this test will be used for prediction of the swelling behavior of the MHW and GPHS heat sources under an internal pressure generating from a release of helium from PuO_2 fuel. The specimens were heat treated 19 h at 1500°C prior to tensile testing. The tensile results are obtained as follows.

Test Temperature (°C)	0.2% Offset Yield Strength (MPa)	(ksi)	Ultimate Tensile Strength (MPa)	(ksi)	Elongation (%)
650	66.8	9.7	521	75.6	31.2
1350	56.5	8.2	149	21.6	49.7
1600	44.1	6.4	115	16.7	50.0

Note that the tensile strength of DOP-26 is higher than that of Pt–30 Rh by about 300% at temperatures above 1350°C.

AES Analysis of P-Doped DOP-26 (C. L. White and R. A. Padgett)

We have previously reported Auger electron spectroscopy (AES) results on P-doped DOP-26 alloy, as part of an ongoing effort to determine the relationship between phosphorus contamination at DOP-26 grain boundaries, and reduced impact ductility at elevated temperatures. Our previous studies have shown that (1) phosphorus contamination can reduce high-temperature-impact (HTI) ductility to almost zero and (2) annealing in vacuum at 1500°C removes phosphorus from the grain boundaries and restores significant levels of ductility in HTI.

We have recently analyzed two additional specimens that had been P-doped at LASL (as had all previous specimens). These specimens were 800036 (DLMF-8C) and 800037 (DLMF-8BC). Specimen 800036 was examined in the "as doped" condition, and Specimen 800037 had been given a 15 min vacuum anneal following P-doping.

AES results on Specimen 800036 were not typical of other "as doped" specimens that we have studied. Phosphorus levels on the freshly fractured specimen were approximately the same as for other "as doped" specimens that we have examined, however there was an additional Auger peak at 183 eV (possibly due to either chlorine or boron). This peak showed some tendency to grow with time. Comparison of two spectra taken in the same location on the sample surface, but at different times, showed the later spectrum to have a larger 183 eV peak and a smaller 120 eV phosphorus peak. One other unusual result from Specimen 800036 is that the oxygen levels indicated by the Auger spectra were significantly larger than normally observed for DOP-26 material.

AES results on Specimen 800037 did not show the large 183 eV peak observed for the previous specimen. Three area analyses (yielding an average surface composition over approximately one-third of the specimen thickness) and 27 point analyses were performed. The average P (120 eV)/ Ir (229) Auger peak height ratio* was 0.475. This value falls between previously reported values for "as doped" specimens, and the value reported for Specimen 800023 (DLMF-8AC, P-doped + 1 H/1500°C/vac). Figure 3 shows a plot of the P/Ir peak height ratio versus vacuum annealing time for the specimens examined to date.

AES Analyses of S-Doped DOP-26 (C. L. White, H. Inouye and R. A. Padgett)

We have previously reported AES results on a DOP-26 specimen (#800029) that had been exposed to sulfur vapor.[2] Large sulfur concentrations were observed on some portions of the intergranular fracture surface and essentially none on others. We have examined an additional specimen, #800033, that was given the same exposure to sulfur as #800029 and then given a 1 h/1500°C/vacuum anneal in an attempt to remove the sulfur. AES analysis of this specimen yielded no evidence of sulfur at the DOP-26 grain boundaries. Because of the nonuniform sulfur coverage on the as exposed specimens it will be necessary to confirm results on both of these specimens before their generality can be assumed.

Characterization of DOP-26 Ir–0.3% W Production Sheet (D. E. Harasyn and C. T. Liu)

The purpose of this subtask is to characterize production lots of Ir–0.3% W sheet. Primarily this involves reporting the results of uniaxial impact tests performed on each production lot. A production lot is normally 48 blanks fabricated from six ingots.

---

*This ratio was obtained in the same manner as for previously reported average peak height ratios[3] except that three rows of nine (rather than ten) points each were analyzed.

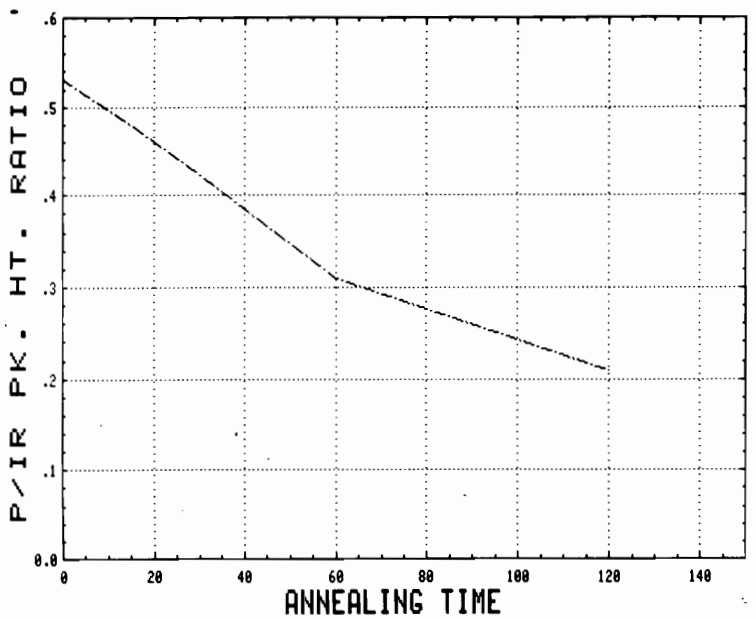

Fig. 3. A Plot of the Auger P/Ir Peak Height Ratio Versus Vacuum Annealing Time for the P-Doped Specimens (DOP-26) annealed at 1500°C.

The tensile impact data presented in Table 4 for recrystallized DOP-26 Ir–0.3% W samples indicate that the material is not sensitive to surface imperfections. The DOP-26 alloy is sensitive to Zr contamination. Note that even as little as 70 μg/g Zr significantly reduces the ductility under the GPHS impact conditions (980°C and 61 m/s). We are examining a heat contaminated with a smaller amount of Zr. We expect to have those results in August.

Sample L275 was contaminated with 200 μg/g Fe, 70 μg/g Cr, and 40 μg/g Ni. This apparent contamination with stainless steel did not affect the ductility of the Ir sheet. Before we recommend the disposition of this material we will impact test a GTA butt weld.

Impact Properties of Pt–30% Rh (H. Inouye)

As part of the GPHS/LWRHU working group request, the impact properties of Pt–30% Rh were determined at 200°C and 48 m/s. Table 5, which lists the ductility and reduction in area versus heat treatment, shows no adverse effect of the heat pulse nor any indications of incompatibility with pyrolytic graphite to 1700°C.

Table 4. Tensile Impact Data on DOP-26 Production Sheets[a]

Sheet No.	Uniform Elongation	Reduction of Area	Fracture Mode[b]	Remarks
WK-12	16.4	25	TF+GBS	
L216 (A1)	18.7	36	TF+GBS	Surface inclusions in gage length
L216 (A2)	19.8	37	TF+GBS	Surface inclusions in gage length
LR238	16.8	—	TF+GBS	
L246	16.7	—	TF+GBS	
L261	15.2	—	TF+GBS	
L264	17.8	26	TF+GBS	C-brale indentions 0.07 mm (0.0028 in.) deep, 1 cm apart in gage length
L268-5	15.5	30	TF+GBS	Linear liquid penetrant indications in gage length
L268-5	14.7	25	TF+GBS	
L272 (A)	7.4	9	GBS	Contaminated with 100 μg/g Zr
L274	9.2	—	GBS	Contaminated with 70 μg/g Zr
L275	18.3	—	TF+GBS	Contaminated with 200 μg/g Fe, 70 μg/g Cr, and 40 μg/g Ni

[a]Samples annealed 19 h at 1500°C, impacted at 61 m/s at 980°C

[b]TF = transgranular fracture, GBS = grain boundary separation

Table 5. Impact Properties of Pt–30% Rh[a] at 200°C and Test Velocity of 48 m/s

Heat Treatment	Elongation (%)	Reduction-in-Area (%)
1 h @ 600°C (stress-relieved)	12.9	79.5
1 h @ 900°C (recrystallized)	29.0	89.7
2 min @ 1600°C (heat pulse)	37.7	∿100
2 min @ 1600°C + pyrolytic graphite	36.4	89.3
2 min @ 1700°C + pyrolytic graphite	37.8	88.7

[a]Sheet supplied by Mound Laboratory.

REFERENCES

2. A. C. Schaffhauser, *Technical Highlights of Space and Terrestrial Systems Programs at Oak Ridge National Laboratory for May 1980*, ORNL/CF-80/258, p. 6.

3. A. C. Schaffhauser, *Technical Highlights of Space and Terrestrial Systems Programs at Oak Ridge National Laboratory for April 1980*, ORNL/CF-80/235, pp. 11–13.

ISOTOPE FUEL DEVELOPMENT

(Activity AE 15 35 00 0, WPAS 02314)

R. S. Crouse

$^{90}SrF_2$ Compatibility (R. S. Crouse)

Due to equipment breakdowns no microprobe analysis was possible in July.

H. T. Fullam requested that we examine the end cap of a $^{90}SrF_2$ capsule from Rockwell-Hanford. This capsule was from Lars Edvaldson, who suspects some laminations in the cap material. The $^{90}SrF_2$ was being sent to the Operations Division of ORNL for pressing into pellets so the capsule was already on site. The cap will be removed by the personnel in the Fission Product Development Laboratory and sent to the HRLEL for our handling.

TERRESTRIAL RADIOISOTOPE APPLICATION DEVELOPMENT

(Activity AE 15 35 00 0. WPAS 01367)

F. N. Case, K. W. Haff, and F. J. Schultz

Cesium-137 Low Solubility Compounds

Leaching of the unsectioned, fully loaded ^{137}Cs aluminosilicate pellets in ∿305K (∿90°F) distilled water was begun this month. The 0.0254 m (1 in.) diam by 0.0286 m (1-1/8 in.) high pellets, each with a surface area of ∿13 cm^2, were immersed in ∿400 ml of distilled water. This static leach test approaches a dynamic experiment by employing frequent sampling periods wherein fresh distilled water is substituted at short time intervals. The leach rates are reported below in Table 6.

Table 6. Unsectioned, Fully Loaded Cesium-137 Aluminosilicate Pellet Leach Rates

Sample No.	Leaching Period Interval (days)	Accumulated Leaching Period (days)	Leach Rate ($kg/m^{-2} \cdot s^{-1}$)
1-1	0.118	0.118	6.79×10^{-9}
1-2	0.110	0.228	3.09×10^{-9}
1-3	0.799	1.027	3.66×10^{-10}
1-4	0.196	1.223	1.35×10^{-10}
1-5	0.756	1.979	4.19×10^{-11}
1-6	0.237	2.216	2.92×10^{-11}
1-7	0.730	2.944	1.07×10^{-11}
1-8	0.210	3.156	1.34×10^{-11}
1-9	0.784	3.90	8.22×10^{-12}
2-1	0.113	0.113	7.16×10^{-9}
2-2	0.108	0.221	2.61×10^{-9}
2-3	0.797	1.018	4.93×10^{-10}
2-4	0.197	1.215	3.94×10^{-10}
2-5	0.756	1.971	7.63×10^{-11}
2-6	0.237	2.208	3.60×10^{-11}
2-7/25	0.731	2.939	2.00×10^{-11}
2-8	0.208	3.147	2.91×10^{-11}
2-9	0.788	3.935	1.91×10^{-11}

The fabrication history of each pellet is given in Table 7.

Table 7. Fabrication History of the Static Leachant Sample Pellets

Pellet No.	Pellet Production Run	^{137}Cs Pollucite Batch No.	Power Reading at Maximum Ram Travel (kW)	Ram Pressure (psig)	Curing Step[a]
1	11	79CsP-5,6,7	19.98	575	30
2	9	79CsP-5,6,7	19.83	595	45

[a]Time power maintained after ram travel had stopped (min).

The leach rates after initial surface decontamination are approximately 100 times lower than for sectioned pellets exposed to refluxing distilled water in a Soxhlet extractor. The grafoil sheath surrounding the whole pellets may, at least partially, account for the lower leach rates observed thus far.

Preliminary results from electron microprobe and electron backscattering examinations of the pollucite pellet sections reveal that no cesium or silicon inhomogeneities exist. That is, both cesium and silicon, two major components of cesium-pollucite, are uniformly distributed throughout the pellet. These results indicate that the cesium/silicon reaction during hot pressing was complete.

Leaching of the sectioned, fully loaded ^{137}Cs aluminosilicate pellets in the Soxhlet extractors continued this month. The leach rates of each pellet are given in Table 8.

The tracer level ^{137}Cs aluminosilicate pellet sections, which were being leached in the Soxhlet extractors, were removed and exposed to an intense, high energy (^{60}Co:γ_1 = 1.3325 MeV; γ_2 = 1.1732 MeV) gamma-ray field (206,000 R/h) for 100 h. The total dose of 2.06×10^7 R simulated the environment into which the pellets would be positioned in a sludge irradiator. The new leach rates will be compared to those measured prior to exposure to the intense radiation field. This information will be useful in determining the effect of a high energy gamma-ray field on the integrity of the aluminosilicate pellets.

Table 8. Leach Rates of Fully Loaded Cesium-137 Aluminosilicate Pellets

Sample No.	Leaching Period Interval (days)	Accumulated Leaching Period (days)	Leach Rate ($kg/m^{-2} \cdot s^{-1}$)
5-3/25	2.906	6.861	9.41×10^{-10}
5-4/25	4.905	11.766	2.33×10^{-9}
5-5/25	2.913	14.679	2.49×10^{-9}
5-6/25	4.905	19.584	2.81×10^{-9}
5-7/25	7.911	27.495	1.80×10^{-11}
6-3/25	2.906	6.861	1.67×10^{-9}
6-4/25	4.905	11.766	2.04×10^{-9}
6-5/25	2.913	14.679	2.34×10^{-9}
6-7/25	7.911	27.495	2.65×10^{-9}
7-3/25	2.906	6.861	6.15×10^{-10}
7-4/25	4.905	11.766	7.34×10^{-10}
7-5/25	2.913	14.679	1.01×10^{-9}
7-6/25	4.905	19.584	7.27×10^{-10}
7-7/25	7.911	27.495	1.02×10^{-9}
7-8/25	5.898	33.393	1.38×10^{-9}
8-3/25	2.906	6.861	2.96×10^{-9}
8-4/25	4.905	11.766	3.62×10^{-9}
8-5/25	2.913	14.679	3.38×10^{-9}
8-6/25	4.905	19.584	3.41×10^{-9}
8-8/25	5.898	33.393	3.48×10^{-9}

Krypton-85 Light Source Development

A demonstration of the ^{85}Kr light sources was conducted at Andrews Air Force Base, Maryland during the week of July 14-17, 1980. The test results indicate a need for redesigning the light pipe to eliminate a directional problem for better side viewing of the lights. A new light pipe is being designed to eliminate this problem. A revised program plan for the light source development has been written.

BENEFICIAL APPLICATIONS OF RADIATION TECHNOLOGY

(Activity AE 15 35 00 0, WPAS BART001)

C. S. Sims

The preliminary draft BART program plan was issued on July 9.

The second draft of the ORNL assessment of the ^{137}Cs irradiation technology program was distributed on July 15 in preparation for final review at DOE-Germantown on July 30-31. The review was attended by 22 persons representing 6 different concerned organizations. The document was thoroughly reviewed and is to be issued in final form by August 22.

Dr. Edward Josephson of the Massachusetts Institute of Technology held a seminar at ORNL on July 24 on the subject of health aspects of food irradiation.

INTERNAL DISTRIBUTION

1. E. E. Bloom
2. C. R. Brinkman
3. J. A. Carter
4. F. N. Case
5–10. R. H. Cooper
11. R. S. Crouse
12. J. E. Cunningham
13. S. A. David
14. J. H. DeVan
15. R. G. Donnelly
16. W. P. Eatherly
17. J. I. Federer
18. G. M. Goodwin
19. K. W. Haff
20. J. P. Hammond
21. W. O. Harms
22. R. L. Heestand
23. M. R. Hill
24. J. R. Keiser
25. J. W. Koger
26. H. Inouye
27. E. Lamb
28. C. T. Liu
29. D. L. McElroy
30. C. D. Montgomery
31. T. K. Roche
32. A. C. Schaffhauser
33. C. S. Sims
34. G. M. Slaughter
35. J. O. Stiegler
36. V. J. Tennery
37. D. B. Trauger
38. G. C. Wei
39. J. R. Weir, Jr.
40. C. L. White
41–45. Laboratory Records
46. Laboratory Records, ORNL RC
47. ORNL Patent Office

EXTERNAL DISTRIBUTION

48–59. DOE Space and Terrestrial Systems Division, Washington, DC 20545

G. L. Bennett
R. C. Brouns
F. M. Dieringer
N. Goldenberg
J. S. Griffo
W. D. Kenney
J. J. Lombardo
R. B. Morrow
P. A. O'Riordan
W. C. Remini
B. J. Rock
C. O. Tarr

60–61. DOE Albuquerque Operations Office, P.O. Box 5400, Albuquerque, NM 87115

D. K. Nowlin
D. Plymale

62–63. DOE Oak Ridge Operations Office, P.O. Box E, Oak Ridge, TN 37830

J. A. Lenhard
J. Pidkowicz

64–65. DOE San Francisco Operations Office, 1333 Broadway, Wells Fargo Building, Oakland, CA 94612

L. Lanni
W. L. Von Flue

66–67. DOE Savannah River Operations Office, P.O. Box A, Aiken, SC 29801

W. T. Goldston
W. D. Sandberg

68. DOE Dayton Area Office, P.O. Box 66, Miamisburg, OH 45342

H. N. Hill

69. Air Force Weapons Laboratory, Kirtland Air Force Base, DYUS, Albuquerque, NM 87116

Michael Seaton

70–71. Battelle Columbus Laboratories, 505 King Ave., Columbus, OH 43201

E. L. Foster
I. M. Grinberg

72–73. E. I. du Pont de Nemours, Savannah River Plant, Aiken, SC 29801

R. A. Brownback
W. R. Kanne

74–75. E. I. du Pont de Nemours, Savannah River Laboratory, Aiken, SC 29801

R. L. Folger
R. H. Tait

76–77. Fairchild Industries, 20301 Century Blvd., Germantown, MD 20767

M. Eck
A. Schock

78. General Atomic Co., P.O. Box 81608, San Diego, CA 92138

N. B. Elsner

79–81. General Electric Co., Valley Forge Space Center, P.O. Box 8048, Philadelphia, PA 19101

V. Haley
R. J. Hemler
C. W. Whitmore

82–84. Jet Propulsion Laboratory, California Institute of Technology, 4800 Oak Grove Drive, Pasadena, CA 91103

R. W. Campbell
J. E. Mondt
A. E. Wolfe

85. Johns Hopkins University, Applied Physics Laboratory, Johns Hopkins Road, Laurel, MD 20810

J. C. Hagan

86–88. Los Alamos National Scientific Laboratory, P.O. Box 1663, Los Alamos, NM 87545

S. E. Bronisz
S. S. Hecker
W. J. Maraman

89–91. Minnesota Mining and Manufacturing Co., St. Paul, MN 55101

R. B. Ericson
J. D. Hinderman
W. C. Mitchell

92–93. Monsanto Research Corp., P.O. Box 32, Miamisburg, OH 45342

E. W. Johnson
W. C. Wyder

94. Sundstrand Energy Systems, 4747 Harrison Ave., Rockford, IL 61101

E. Krueger

95–96. Teledyne Energy Systems, 110 W. Timonium Rd., Timonium, MD 21093

W. J. Barnett
W. E. Osmeyer